315 (2026) 106565

Contents lists available at ScienceDirect

The Veterinary Journal

journal homepage: www.elsevier.com/locate/tvjl

Evaluation of [^{18}F]FAPI-74 PET/CT in healthy dogs and in West Highland white terriers with canine idiopathic pulmonary fibrosis: a pilot study

Elodie Rizzoli [a,*], Mohamed Ali Bahri [b], Sylvestre Dammicco [b], Christian Degueldre [b], Alexandru Tutunaru [a], Mutien-Marie Garigliany [c], Mazarine Gérardy [c], Géraldine Bolen [a], Nadia Withofs [b,d], Thibault Gendron [b], Cécile Clercx [a]

[a] Department of Companion Animals Clinical Sciences, Faculty of Veterinary Medicine, University of Liege, Liege 4000, Belgium
[b] GIGA CRC Human Imaging, University of Liège, Liège 4000, Belgium
[c] Department of Morphology and Pathology, Faculty of Veterinary Medicine, University of Liege, Liege 4000, Belgium
[d] Division of Nuclear Medicine and Oncological Imaging, Department of Medical Physics, CHU of Liege, Liege 4000, Belgium

ARTICLE INFO

Keywords:
Dog
Lung
Idiopathic pulmonary fibrosis
Fibroblast activation protein
West highland white terriers
PET/CT

ABSTRACT

Canine idiopathic pulmonary fibrosis (CIPF) is a fatal disease affecting primarily West Highland white terriers (WHWT). CIPF remains challenging to diagnose and disease progression is difficult to predict. Recently, fibroblast activation protein (FAP) was identified as a cellular marker of active fibrosis in post-mortem lung biopsies from CIPF-affected WHWTs. Therefore, FAP-targeted imaging using FAP inhibitors (FAPI) may offer a noninvasive means of assessing active fibrosis in canine lungs in vivo. This study aimed to evaluate whether [^{18}F]FAPI-74 positron emission tomography (PET) combined with computed tomography (CT) can detect FAP expression in the lungs of CIPF-affected WHWTs. This prospective exploratory pilot study included two healthy senior purpose-bred Beagle dogs and two client-owned WHWTs diagnosed with CIPF. In addition to CT, each dog underwent a 90-min dynamic thoracic PET scan following intravenous administration of [^{18}F]FAPI-74 (median activity 10.3 MBq/kg). In one Beagle and one WHWT, a subsequent static abdominal PET scan was performed to assess biodistribution. PET and CT images were co-registered prior to quantitative uptake analysis. [^{18}F]FAPI-74 PET was well tolerated in all dogs and compatible with clinical use. [^{18}F]FAPI-74 uptake was approximately three-fold higher in CIPF-affected lungs than in healthy lungs. Tracer elimination occurred via both urinary and hepatobiliary routes. Moderate uptake was also observed in gastrointestinal organs, potentially reflecting age-related fibrosis, as supported by additional immunohistochemistry. In conclusion, [^{18}F]FAPI-74 PET/CT enables in vivo detection of active pulmonary fibrosis in CIPF-affected dogs and represents a promising noninvasive tool for detecting and monitoring this fatal disease.

1. Introduction

Canine idiopathic pulmonary fibrosis (CIPF) is an interstitial lung disease of unknown etiology that particularly affects senior West Highland White Terriers (WHWTs) (Clercx et al., 2018; Laurila and Rajamäki, 2020). It leads to progressive respiratory failure, ultimately resulting in death or euthanasia (Heikkilä et al., 2011). Diagnosis is based on the exclusion of other diseases and typically involves a combination of tests, including a 6-minute walk test, arterial blood gas analysis, complete blood analysis, echocardiography, bronchoscopy with bronchoalveolar lavage, thoracic radiography, and, most importantly, computed tomography (CT) of the thorax (Heikkilä et al., 2011; Lilja-Maula et al., 2014; Roels et al., 2017; Thierry et al., 2017). A definitive diagnosis requires histopathological examination, which is most often conducted post-mortem (Heikkilä et al., 2011; Syrjä et al., 2013). Given the absence of curative treatment, the prognosis for CIPF remains poor, with median survival times between 7 and 11 months from diagnosis (Lilja-Maula et al., 2014; Thierry et al., 2017; Corcoran et al., 1999). The variability in disease progression among individuals and the lack of prognostic biomarker make it challenging to predict disease progression (Clercx et al., 2018; Laurila and Rajamäki, 2020).

Humans can also develop fibrotic interstitial lung diseases of unknown cause, the most frequent being idiopathic pulmonary fibrosis (IPF) (Raghu et al., 2022). IPF primarily affects older adults, leads to

* Correspondence to: Avenue de Cureghem n°1, Liège 4000, Belgium.
E-mail address: elodie.rizzoli@uliege.be (E. Rizzoli).

https://doi.org/10.1016/j.tvjl.2026.106565
Received 11 October 2025; Received in revised form 13 January 2026; Accepted 13 January 2026
Available online 15 January 2026

respiratory insufficiency, and carries a poor prognosis (Raghu et al., 2022). Recently, new modalities have been developed for the noninvasive assessment of fibrotic interstitial lung diseases by targeting in vivo fibroblast activation protein (FAP), a marker of activated fibroblasts (Acharya et al., 2006; Yang et al., 2023). FAP inhibitors (FAPI), radiolabeled with Gallium-68 (^{68}Ga) or Fluorine-18 (^{18}F), are used as radiotracers for positron emission tomography (PET), often combined with CT (PET/CT) (Röhrich et al., 2022; Yang et al., 2023; Mori et al., 2024; Hotta et al., 2024). FAP-targeted PET/CT imaging shows an increased uptake in IPF, indicating active fibrogenesis, being correlated with CT findings and disease severity, and potentially predicting disease progression (Röhrich et al., 2022; Yang et al., 2023; Mori et al., 2024; Hotta et al., 2024). Compared to ^{18}Ga-labeled compounds, ^{18}F-labeled agents such as [^{18}F]FAPI-74 enable centralized large-scale production, provide better spatial resolution, and result in a slightly lower radiation burden (Giesel et al., 2021). Unlike [^{18}F]fluorodeoxyglucose ([^{18}F]FDG), a more commonly used radiotracer which targets high glucose metabolism, including in lung fibrotic lesions, [^{18}F]FAPI-74 is more specific for fibrogenesis, causes less physiological background uptake and thus provides better contrast, as well as a lower radiation burden (Groves et al., 2009; Giesel et al., 2021; Röhrich et al., 2022).

As in humans, FAP-targeted PET/CT could constitute a new noninvasive diagnostic tool to detect activated fibroblasts in CIPF and potentially predict disease progression or evaluate response to therapy. FAP expression has recently been described in areas of active fibrosis in post-mortem lung biopsies from CIPF-affected dogs (Rizzoli et al., 2024) but has never been investigated in canine lungs in vivo. Furthermore, there is no available data on [^{18}F]FAPI-74 pharmacokinetics in dogs. In veterinary medicine, PET imaging is gaining popularity for clinical and research applications (LeBlanc and Morandi, 2014; LeBlanc and Peremans, 2014; Randall, 2016). Despite limited PET(/CT) availability in veterinary settings, collaborations with human medical institutions enable imaging of veterinary patients (LeBlanc and Morandi, 2014). Combining the molecular insights of PET with the anatomical precision of CT makes PET/CT a powerful tool for diagnosis and staging (LeBlanc and Peremans, 2014; Randall, 2016; Maitz et al., 2022).

This study aimed to assess the safety and feasibility of [^{18}F]FAPI-74 PET in dogs, and to explore its ability to detect in vivo FAP expression in CIPF-affected versus healthy lungs, hypothesizing increased [^{18}F]FAPI-74 uptake in diseased lungs only.

2. Materials and methods

2.1. Case selection

This prospective exploratory pilot study included two healthy senior purpose-bred Beagle dogs (Control1 and Control2) with no history of lung disease, no clinical sign, and normal physical examination including cardiorespiratory auscultation. In addition, two client-owned WHWTs previously diagnosed with CIPF (CIPF1 and CIPF2) were included, with owner's written informed consent. CIPF diagnosis was established prior to enrollment, based on a 6-minute walk test, hematology and serum biochemistry, arterial blood gas analysis, echocardiography, thoracic CT, and endoscopy with bronchoalveolar lavage (Clercx et al., 2018; Laurila and Rajamäki, 2020).

2.2. Computed tomography

In all dogs, non-enhanced CT was performed with a 64-multislice CT scanner (Somatom Confidence 64, Siemens, Germany). For Beagle dogs, the acquisition parameters were as follows: voltage 100 kV, reference current 212 mA modulated by automatic exposure control (Care Dose, Siemens), pitch 0.8, reconstructed with a 0.75-mm slice thickness. For WHWTs, the acquisition parameters were as follows: voltage 100 kV, reference current 170 mA modulated by automatic exposure control (Care Dose, Siemens), pitch 1.2, reconstructed with a 1-mm slice thickness. CT images were acquired under general anesthesia, except for one case (CIPF1), which was performed under mild sedation with 0.3 mg/kg IV of butorphanol due to a prior CT examination already performed under general anesthesia. In all cases performed under general anesthesia, images obtained during the expiratory pause were selected for analysis.

2.3. [^{18}F]FAPI-74 production

[^{18}F]FAPI-74 radiotracer was synthesized on an AllInOne synthesizer using production cassette and reagent kit from TRASIS (Ans, Belgium). The precursor and ^{19}F reference were provided by SOFIE iTheranostics (Dulles, VA). The radioactivity of the [^{18}F]FAPI-74 solution was 5.1 ± 0.5 GBq with a decay-corrected yield of 66 ± 7 %. The molar activity of 94 ± 20 GBq/μmol was measured after radiosynthesis with a purity of 99.5 ± 0.1 %. Final solution was diluted with saline to reach a volume of injection between 2 and 3 mL per dog.

2.4. [^{18}F]FAPI-74 positron emission tomography

For PET imaging, the dogs were premedicated 0.3 mg/kg IV of butorphanol and general anesthesia was induced with midazolam 0.2 mg/kg IV and propofol IV titrated to effect and maintained with isoflurane 1.5 % in oxygen by an endotracheal tube. A urinary catheter was placed to prevent radioactive contamination, and the dogs were positioned in sternal recumbency for the imaging session, under spontaneous ventilation by a rebreathing system. Respiratory rate, heart rate, hemoglobin oxygen saturation, end-tidal CO_2 and arterial blood pressure were continuously measured throughout the procedure using a multiparameter monitor (HS-VPM-15, Henry Schein, Melville, NY) and recorded every 5 min. PET images were acquired using a Siemens/CTI (Knoxville, TN) ECAT EXACT HR+ scanner with a 15-cm field of view, without respiratory gating. Before the radiotracer was injected, a 10-minute transmission scan using a Germanium-68 (^{68}Ge) source was performed to create a reference image for attenuation correction.

The [^{18}F]FAPI-74 radiotracer was injected as an intravenous bolus via the saphenous vein. The median injected activity was 10.3 MBq/kg (8.1–20.6 MBq/kg). Dynamic PET imaging of the thorax was performed using a series of time frames – 6 of 10 s, 8 of 30 s, 5 of 120 s, and 15 of 300 s – resulting in a total acquisition duration of 90 min. In Control2 and CIPF1, thoracic imaging was followed by a static 5-min abdominal acquisition for assessment of tracer biodistribution and elimination pathways. Table 1 summarizes patient, injection and acquisition parameters. All PET images were reconstructed using filtered back projection with a voxel size of 2,57 × 2,57 × 2,43 mm and corrections for measured attenuation, dead time, random events, and scatter using standard software (ECAT 7.1, Siemens/CTI, Knoxville, TN).

At the end of the procedure, the dogs were moved to a 2.4 m^2 open pen. Once awake, their bladders were emptied and the urinary catheters were removed. The dogs were cleared to return to the kennel or home when the radioactive dose rate, measured with a Geiger-Müller counter at a 1-meter distance, dropped below the national regulatory threshold of 20 μSv/h.

2.5. Image analysis

Using PMOD software v4.0, PET images were manually co-registered with CT images using the activity detected in the heart and major blood vessels during the initial post-injection frames as spatial landmark for image alignment. The total volume of both lungs (total lung volume; TLV) was segmented semi-automatically based on CT images. Regions of interest (ROIs), represented by 12-mm diameter spheres, were drawn on PET images, under CT images guidance. ROIs were placed in each lobe of both lungs, in areas that are standardized across all dogs and previously used in CIPF studies (Rizzoli et al., 2024): in the periphery of the right cranial lobe (A1) and cranial part of the left cranial lobe (B1); centrally,

Table 1
Patient, injection and acquisition parameters for [^{18}F]FAPI-74 PET scans.

Case	Age (years)	Breed	Gender	Weight (kg)	Injected activity (MBq/kg)	Scanned regions
Control 1	10	Beagle	Intact female	10.7	20.6	Thorax
Control 2	10	Beagle	Intact female	14.1	10.7	Thorax Abdomen
CIPF 1	14	WHWT	Intact male	9.3	9.9	Thorax Abdomen
CIPF 2	10	WHWT	Neutered female	10.0	8.1	Thorax

FAPI: fibroblast activation protein inhibitor; PET: positron emission tomography; CIPF: canine idiopathic pulmonary fibrosis; WHWT: West Highland white terrier.

near the hilum, in the right middle lobe (A2) and in the caudal part of the left cranial lobe (B2); caudo-dorsally (A3 and B3) and ventro-laterally (A4 and B4) in the right and left caudal lobes; and in the periphery of the accessory lobe (A5). Additional ROIs were drawn on other identifiable anatomical structures within the field of view, including thoracic aorta, caudal vena cava, esophagus, right and left ventricles, 5th thoracic vertebra (T5), paravertebral muscle (lateral to T5), cranial and medial liver, gallbladder, gastric wall and kidneys.

Mean (SUV_{mean}) and maximal (SUV_{max}) standardized uptake values were measured for each ROI and TLV. SUVs were calculated voxel-by-voxel as the product of the activity concentration in the image (Bq/mL) divided by the injected dose (Bq), multiplied by the dog's body weight (kg) and a factor of 1000. SUV_{mean} was defined as the average SUV of all voxels within the ROI, whereas SUV_{max} was defined as the SUV of the voxel with the highest value within the ROI. Target-to-background ratios (TBR) were calculated by dividing SUV_{mean} of the ROI by SUV_{mean} of the paravertebral muscle, serving as background reference. Mean Hounsfield units (HU_{mean}) were measured on CT images for lung ROIs and TLV.

To quantify parameters reflecting the lung distribution pattern of the tracer, an approach adapted from a study in human patients (Yang et al., 2023) was used. Specifically, the SUV_{mean} of the aorta, representing the mediastinal blood pool activity, was used as an absolute threshold to segment the TLV, within which all voxels with SUV values exceeding this threshold defined the total active volume (TAV) (Yang et al., 2023). To account for size difference between dog breeds, TAV was expressed as a percentage of TLV (TAV%). Finally, TAV% was multiplied by the SUV_{mean} of TAV to obtain the SUV_{total} (Yang et al., 2023). Due to the small pilot sample, all group comparisons were reported descriptively using medians and ranges of individual values.

2.6. Immunohistochemistry

Since [^{18}F]FAPI-74 uptake was detected in unexpected tissues, such as the gastric wall, FAP expression was further investigated by immunohistochemistry. Full thickness gastric wall biopsies were collected post-mortem from the fundus, greater curvature, and antrum of additional dogs euthanized for unrelated medical reasons, with owner consent. Biopsies were formalin-fixed, paraffin-embedded, and routinely processed for histopathological evaluation using hematoxylin and eosin staining. Adjacent 5-µm sections were deparaffinized, and rehydrated, and subjected to antigen retrieval by Tris-EDTA (10 mM Tris, 1 mM EDTA, pH 8.5–9.0) incubation in microwave for 15 min at 600 W. Endogenous peroxidase activity was blocked with 3 % hydrogen peroxide incubation for 30 min. Nonspecific binding was blocked by incubation in blocking buffer (Vector Laboratories #SP-5035–100) for 30 min. Sections were incubated overnight at 4°C with rabbit anti-human FAP monoclonal antibody (Abcam #ab207178, 1:100) validated for dogs (Rizzoli et al., 2024). For specificity control, the primary antibody was substituted with isotype rabbit IgG antibody (Enzo #ENZ-ABS491–0200, 1:200). Sections were incubated with peroxidase-labeled polymer goat anti-rabbit antibody (Dako #K4003) for 30 min at room temperature, followed by AEC (ImmPACT #SK-4205) for 12 min and hematoxylin counterstaining. FAP expression was evaluated by two observers (including a diplomate of the European College of Veterinary Pathologists) and each case was globally graded as negative (no detectable staining), mild (staining in less than 10 % of fibroblasts), moderate (staining in 10–50 % of fibroblasts), or severe (staining in more than 50 % of fibroblasts).

3. Results

3.1. Clinical and diagnostic findings

Both Beagle dogs presented no clinical signs, had normal lung auscultation and showed no abnormalities on CT scans. One year after PET images acquisition, Control1 was euthanized for unrelated medical reasons, which allowed the collection of post-mortem lung biopsies to confirm the absence of lung disease at that time. At diagnosis, both CIPF1 and CIPF2 had a history of chronic dry cough and expiratory dyspnea and presented diffuse inspiratory lung crackles at lung auscultation. CIPF1 also had episodes of syncope, whereas CIPF2 exhibited exercise intolerance. Complete diagnostic work-up in both dogs revealed unremarkable hematology, biochemistry, and electrolyte analyses; however, severe and moderate hypoxemia were present, with arterial partial pressure of oxygen of 56.6 mmHg in CIPF1 and 61.4 mmHg in CIPF2, respectively. Six-minute walk distance was 308.7 m for CIPF1 and 434.7 m for CIPF2. Both dogs had a high probability of moderate pulmonary hypertension according to ACVIM guidelines (Reinero et al., 2020), as indicated by a systolic pulmonary arterial pressure estimated at 50 mmHg in CIPF1 and 47 mmHg in CIPF2 and echocardiographic signs of pulmonary hypertension in at least one anatomic site. Thoracic computed tomography in both dogs showed diffuse ground-glass opacities in a mosaic pattern; CIPF2 additionally exhibited parenchymal bands. Bronchoscopy findings included bronchiectasis and bronchomalacia. Bronchoalveolar lavage fluid analysis revealed an increased leukocyte count (1880 cells/µL with 82 % macrophages in CIPF1; 840 cells/µL with 95 % macrophages in CIPF2).

3.2. Safety and radiation dosimetry

Following the injection of [^{18}F]FAPI-74, no alterations in anesthetic monitoring parameters were observed. One hour after the injection, the urine collected from Control1 contained 28 MBq of [^{18}F] activity, corresponding to 20 % of the injected activity (decay corrected). Control1 remained above the 20 µSv/h dose-rate threshold for 2.5 h after receiving 20.6 MBq/kg of [^{18}F]FAPI-74. After protocol refinement and injection of approximately 10 MBq/kg in subsequent dogs, restricted-area confinement was unnecessary as Control2 had a radioactive dose rate below 20 µSv/h by the end of the thoracic imaging and both WHWTs were below this threshold within one hour of injection.

3.3. [^{18}F]FAPI-74 uptake

Fig. 1 illustrates the dynamic evolution of lung [^{18}F]FAPI-74 uptake, quantified by SUV_{mean} and TBR, for TLV in all dogs, as well as for lung ROIs in CIPF-affected dogs. Based on this preliminary study, a 60-min uptake time, shown to be optimal for FAP-targeted PET scans in human patients with IPF (Röhrich et al., 2022; Yang et al., 2023; Mori et al., 2024; Hotta et al., 2024), also appears suitable for dogs. This

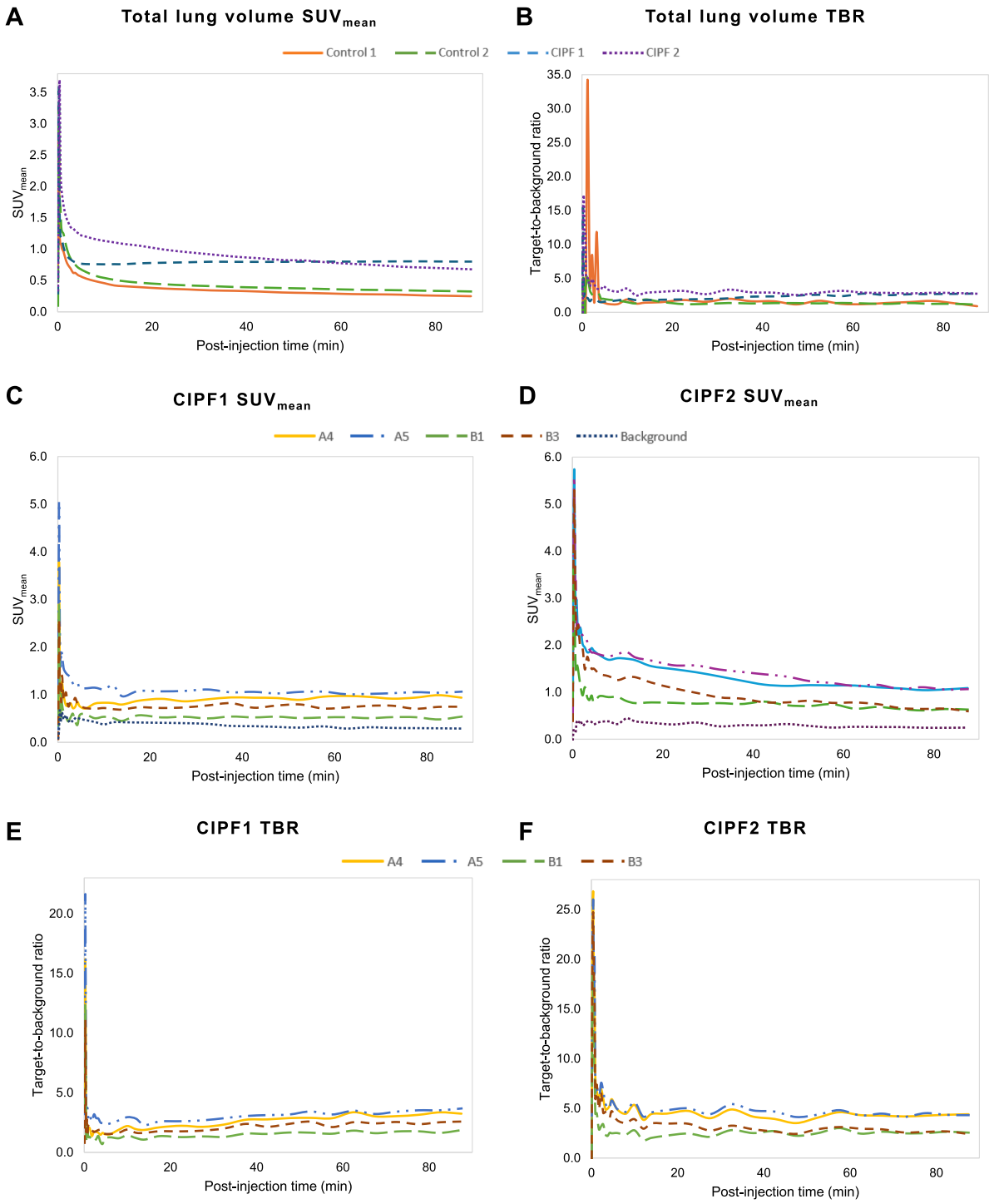

Fig. 1. [^{18}F]FAPI-74 lung uptake curves over the dynamic phase of the study (90 min). Evolution of (A) SUV_{mean} and (B) TBR of total lung volume for the four dogs; evolution of SUV_{mean} (C-D) and TBR (E-F) in specific lung areas (A4, A5, B1, B3 – selected for their distinct uptake curves) within both lungs of CIPF1 and CIPF2. The lung areas were located: in the latero-ventral region of the right caudal lobes (A4); in the periphery of the accessory lobe (A5); in the periphery of the cranial part of the cranial left lobe (B1); in the dorso-caudal region of the left caudal lobe (B3). Increased signal in the first frames reflects first-pass transit of [^{18}F]FAPI-74 through the pulmonary circulation. SUV: standardized uptake values; TBR: target-to-background ratio; CIPF: canine idiopathic pulmonary fibrosis.

time-point allows for sufficient background signal reduction while preserving adequate uptake. Additionally, a 60-min uptake time is practical for clinical use. In all CIPF lung ROIs, [^{18}F]FAPI-74 uptake was higher than background activity (paravertebral muscle).

Representative images of lung [^{18}F]FAPI-74 uptake 60 min post-injection are shown in Fig. 2. All uptake parameters, as well as Hounsfield unit values, were higher in CIPF-affected WHWTs compared with control dogs (Table 2). In all dogs, the cranial abdomen appeared on thoracic PET images and in one dog per group, static abdominal PET images were acquired 90 min post-injection. In all dogs, urinary and hepato-biliary elimination of [^{18}F]FAPI-74 were observed, as evidenced by high activity in the urinary bladder (SUV_{mean} 29.6 in CIPF1), the kidneys (SUV_{mean} 6.6 [4.5–6.9] in the right kidney) and the gallbladder (SUV_{mean} 12.0 [11.6–23.6]), along with moderate activity in the liver

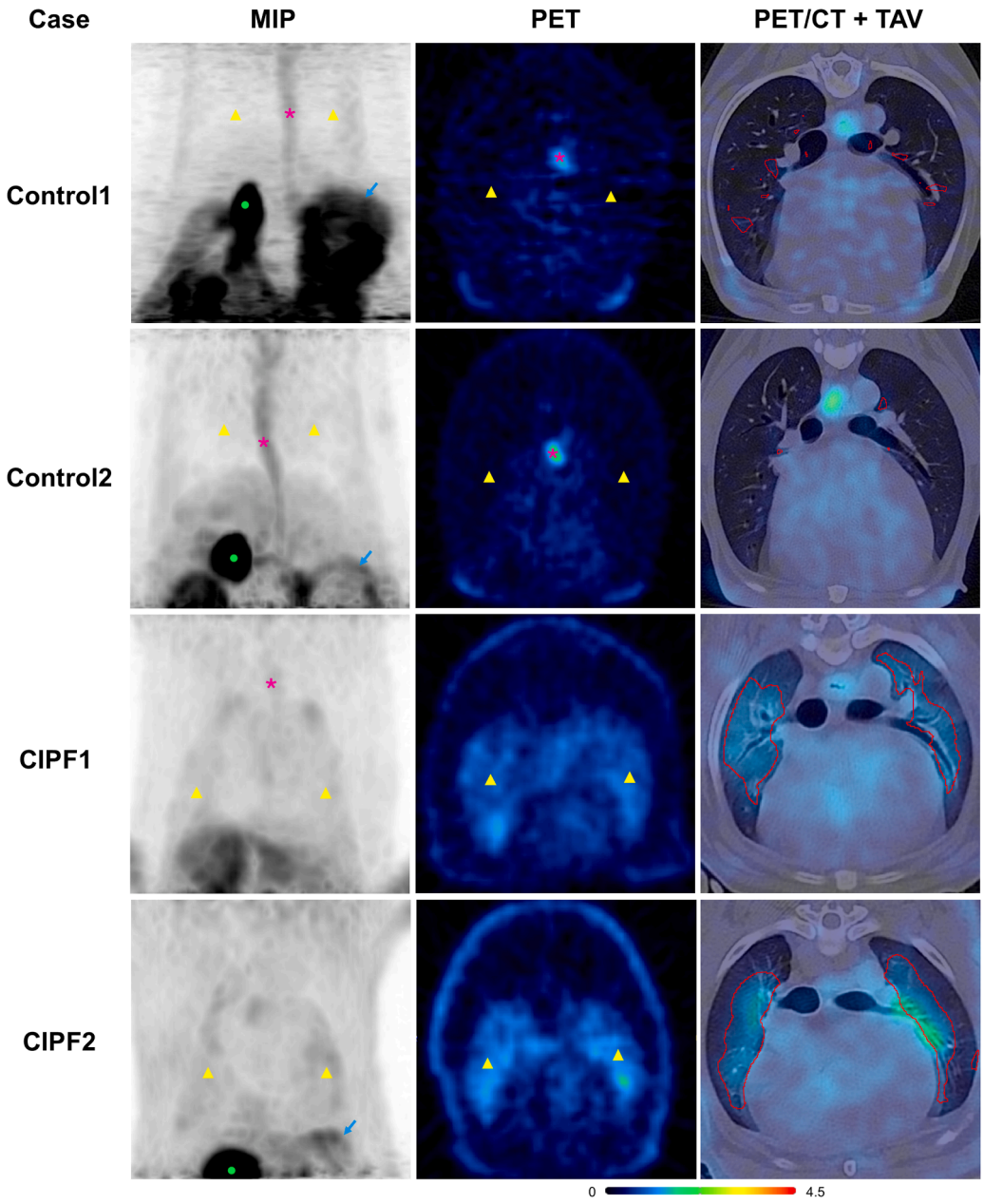

Fig. 2. [^{18}F]FAPI-74 lung uptake in healthy dogs (Control1 and Control2) and in CIPF-affected WHWTs (CIPF1 and CIPF2) 60 min after injection. From left to right, the uptake is represented by maximum intensity projection (MIP) images in dorsal plane, PET images in transverse plane at the level of the 7th thoracic vertebra, PET and CT (pulmonary window) fusion images in transverse plane at the level of the 5th thoracic vertebra, with delineation of the total active volume (red line). MIP images display the highest-intensity signals along each line of sight through the body, providing a 3D-like overview that highlights areas of high tracer uptake. PET images are corrected for attenuation and displayed at a SUV scale of 0–4.5. Yellow triangle: lung; pink star: esophagus; green dot: gallbladder, blue arrow: gastric wall. Of note, Control1 was positioned too cranially, thus a large portion of the cranial abdomen is in the field of view. PET: positron emission tomography; CT: computed tomography.

(SUV_{mean} 1.2 [0.7–2.1]). A moderate uptake was also detected in the gastrointestinal tract of all dogs, particularly in the gastric wall (SUV_{mean} 2.3 [0.7–3.1]), the intestines (SUV_{mean} 3.0 [2.9–3.0] in Control2 and CIPF1) and the esophagus (SUV_{mean} 1.1 [0.7–2.1]). The uptake in abdominal organs of CIPF1 is illustrated in Fig. 3.

3.4. Confirmation of additional FAP expression

Table 3 summarizes the clinical and histopathological characteristics of cases assessed for FAP expression via immunohistochemistry on gastric wall biopsies. FAP was expressed by fibroblasts from the lamina propria and muscularis mucosae in dogs with various levels of gastric fibrosis, even in the absence of gastrointestinal clinical signs (Fig. 4).

4. Discussion

[^{18}F]FAPI-74 PET is a safe and feasible technique in dogs. Importantly, after dose adjustment, confinement was no longer necessary beyond the 60-min uptake time, which appears as an optimal acquisition time-point. [^{18}F]FAPI-74 uptake was increased in CIPF-affected lungs, compared with healthy lungs. Urinary and hepatobiliary elimination of [^{18}F]FAPI-74 was observed, creating a physiological activity in the gallbladder, liver, kidneys and urinary bladder. Additionally, all dogs showed variable moderate uptake in gastrointestinal organs, likely

Table 2
[^{18}F]FAPI-74 lung uptake data 60 min after injection, in control and in CIPF-affected dogs.

	Control (n=2)	CIPF-affected (n=2)
Region of interest (ROI) "A4"		
• **SUV_{mean}**	0.3 (0.3 for both)	1.1 (1.0-1.1)
• **SUV_{max}**	0.5 (0.4-0.6)	1.4 (1.1-1.6)
• **Target-to-background**	1.2 (1.1-1.3)	3.8 (3.4-4.3)
• **Mean attenuation, HU**	-754 (-804 to -704)	-591 (-629 to -553*)
Total lung volume (TLV), mL	424 (263-585)	223 (202-244)
• **SUV_{mean}**	0.3 (0.3-0.4)	0.8 (0.8 for both)
• **SUV_{max}**	2.2 (1.6-2.8)	2.3 (1.8-2.9)
• **Target-to-background**	0.8 (0.4-1.2)	2.8 (2.8-2.9)
• **Mean attenuation, HU**	-772 (-789 to -756)	-600 (-632 to -568*)
Total active volume (TAV), mL	36 (31-41)	110 (88-132)
• **TAV%**	9.4 (7.0-11.9)	48.6 (43.2-54.0)
• **SUV_{mean}**	0.7 (0.5-0.9)	1.0 (1.0 for both)
• **SUV_{total}**	6.2 (6.0-6.4)	48.7 (42.3-55.1)
• **Mean attenuation, HU**	-773 (-773 to -772)	-564 (-604 to -523*)

Data are expressed as medians and ranges of individual values. In this table, [^{18}F]FAPI-74 lung uptake was illustrated in TLV, TAV and one ROI (A4), positioned ventrolaterally in the right caudal lung lobe in each dog. This ROI was selected due to its sufficient distance from adjacent organs, such as the liver, that could artifactually elevate lung uptake values, particularly SUV_{max} in TLV. Target-to-background ratio was calculated by dividing the SUV_{mean} of TLV by the SUV_{mean} of the paravertebral muscle. TAV% was calculated as the TAV divided by the TLV, expressed as a percentage. SUV_{total} is the multiplication of TAV% by the SUV_{mean} of TAV. FAPI: fibroblast activation protein inhibitor; CIPF: canine idiopathic pulmonary fibrosis; WHWTs: West Highland white terriers. *Hounsfield unit (HU) values from CIPF1 were measured on CT images acquired under mild sedation with 0.3 mg/kg of butorphanol.

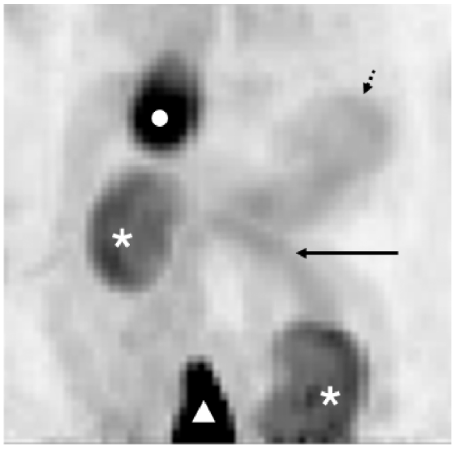

Fig. 3. Maximum intensity projection image depicting [^{18}F]FAPI-74 uptake in the abdomen of CIPF1 90 min after tracer injection. As in other dogs, high activity was detected in the gallbladder (white dot; SUV_{mean} 11.6 and SUV_{max} 13.6), the kidneys (white stars; SUV_{mean} 6.6 and SUV_{max} 7.6 for the right; SUV_{mean} 6.3 and SUV_{max} 7.9 for the left) and the urinary bladder (white triangle; SUV_{mean} 29.6 and SUV_{max} 41.0), along with moderate activity in the gastric wall (dotted arrow; SUV_{mean} 3.1 and SUV_{max} 3.7) and the intestines (full arrow; SUV_{mean} 3.1 and SUV_{max} 3.9).

associated with fibrosis based on immunostaining findings.

This pilot study revealed a marked, approximately 3-fold increase in [^{18}F]FAPI-74 uptake in the lungs of CIPF-affected dogs compared with controls, mirroring findings in human IPF (Röhrich et al., 2022; Yang et al., 2023; Mori et al., 2024; Hotta et al., 2024). These findings support the potential of FAP-targeted PET/CT imaging as a noninvasive method to evaluate the abundance and spatial distribution of activated fibroblasts in vivo in dogs, and to potentially aid in predicting disease progression (Röhrich et al., 2022; Yang et al., 2023; Mori et al., 2024). Such an approach could help diagnose early CIPF cases, for which the distinction between inactive and active, progressive fibrosis remains challenging. Experimental studies have shown that FAP expression is induced in the early phase of lung fibroblast activation rather than in the late phase of lung fibrosis (Yang et al., 2023). In this context, [^{18}F]FAPI-74 PET imaging could be especially relevant for longitudinal disease monitoring and for the selection and enrolment of CIPF-affected dogs at an early disease stage in clinical trials evaluating response to antifibrotic therapy by noninvasively assessing fibrotic activity (Röhrich et al., 2022). WHWTs are recognized as a naturally occurring model of pulmonary fibrosis and therefore represent a valuable translational bridge between experimental models and human disease (Clercx et al., 2018; Laurila and Rajamäki, 2020). As such, studies performed in this clinically relevant canine model may contribute to improving the understanding and evaluation of molecular imaging biomarkers in pulmonary fibrosis, with potential benefit for future human applications. Beyond fibrotic lung diseases, FAP expression has also been demonstrated in canine lung adenocarcinoma (Rizzoli et al., 2024), suggesting that FAP-targeted PET imaging could additionally hold promise for oncological applications in dogs, as already described in human lung cancer (Giesel et al., 2021).

There was no FAPI uptake [^{18}F]FAPI-74 in lungs from control dogs. The low spatial resolution of PET and the impact of respiratory motion tend to artificially elevate the SUV in pulmonary areas adjacent to the diaphragm, thereby leading to an overestimation of SUV, particularly the SUV_{max}, across the total lung volume.

Urinary elimination appeared to be the main route of excretion of [^{18}F]FAPI-74 in dogs, similar to what has been observed in humans (Giesel et al., 2021; Röhrich et al., 2022; Yang et al., 2023; Mori et al., 2024). Hepatobiliary elimination of FAPI, although less commonly reported, has been previously reported and is believed to be due to the lipophilicity of the NOTA chelator used for chelation of [^{18}F]AlF (Giesel et al., 2021; Mu et al., 2023; Xu et al., 2024).

Unexpectedly, mild to moderate [^{18}F]FAPI-74 uptake was observed in gastrointestinal organs. In a previous [^{18}F]FAPI PET/CT study, esophageal uptake was noted in at least one control Beagle dog, although it was not discussed in the text (Li et al., 2023). Specific gastrointestinal uptake has not been reported in [^{18}F]FAPI-74 studies in humans, although intestinal retention has occasionally been described (Mu et al., 2023). In the present study, FAP expression was detected by immunohistochemistry in a subset of gastric walls exhibiting some degree of fibrosis, which may be reflect subclinical, age-related gastric fibrosis reported in dogs (van der Gaag, 1988; Baum et al., 2007). However, secretion of [^{18}F]FAPI-74 by gastrointestinal glands cannot be excluded at this stage (Jayaprakasam et al., 2021).

This study has its limitations. First, due to its exploratory nature,

Table 3
Summary of cases used for FAP immunohistochemistry on gastric wall biopsies.

Case	Age (years)	Breed	Gastrointestinal signs	Cause of euthanasia	Histopathological diagnosis	FAP expression
1	12	Hovawart	None	Aspiration pneumonia	Normal	negative
2	10	Maltese	None	Mammary tumor	Mild gastric fibrosis	mild
3	16	Beagle	None	Severely impaired locomotion	Mild gastric fibrosis	mild
4	11	Beagle	Vomiting, melena	Terminal CKD	Chronic lymphoplasmacytic gastritis with severe fibrosis	moderate
5	14	WHWT	Vomiting	Terminal CKD	Severe gastric fibrosis	mild
6	11	Beagle	None	Ulcerated mammary tumor	Severe gastric fibrosis	moderate

Case 6 corresponds to Control1, which died a year after the PET study, which allowed post-mortem biopsy collection. FAP: fibroblast activation protein.

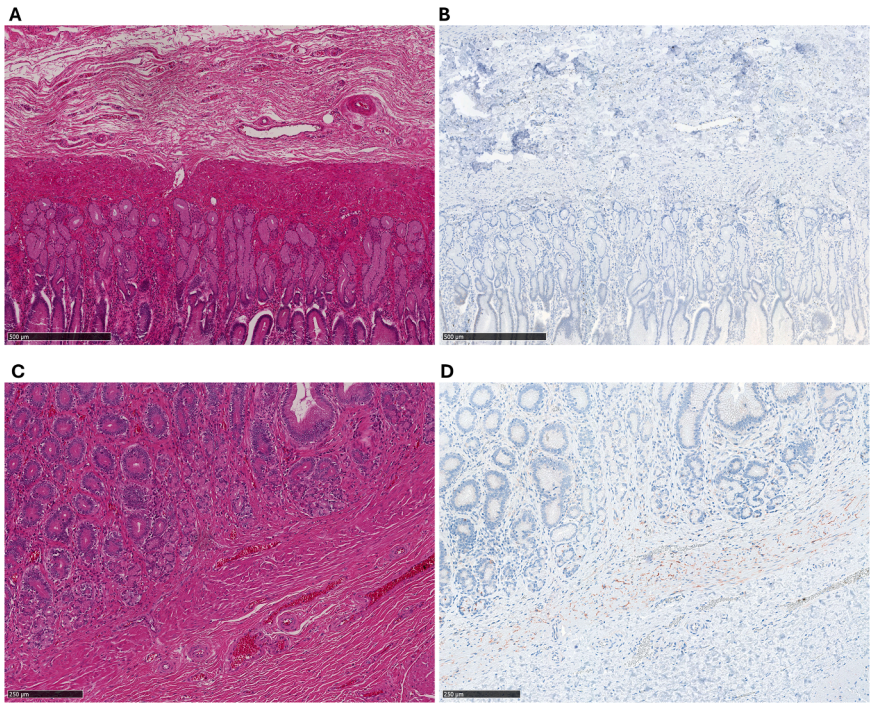

Fig. 4. Panel illustrating FAP expression in canine gastric wall biopsies. Healthy gastric wall in hematoxylin and eosin staining (A) with no FAP expression (B). Gastric wall with gastric fibrosis in hematoxylin and eosin staining (C) with moderate FAP expression (AEC - red staining) in the muscularis mucosae (D).

only four dogs were included. Two Beagle dogs were necessary to refine the imaging procedure and adjust the injected dose before including two privately-owned CIPF-affected WHWTs. While this small sample size was sufficient to assess feasibility and demonstrate the potential of this tool to detect active fibrosis in vivo, a larger study with standardized injected doses is needed to investigate correlations with disease progression or severity. Another limitation is the 15-cm field of view of the PET scanner used for this study, which restricts imaging in large dogs unless static images are acquired at multiple bed positions. Additionally, the lack of respiratory gating contributes to motion-related artifacts. Finally, the use of a hybrid PET/CT scanner instead of stand-alone PET would improve co-registration of PET and CT images, while also reducing anesthesia duration (LeBlanc and Morandi, 2014).

In conclusion, this study demonstrates that [^{18}F]FAPI-74 uptake is observed in the lungs of CIPF-affected dogs, allowing the detection of active fibrosis in vivo. This finding supports the potential of [^{18}F]FAPI-74 PET/CT as a promising noninvasive tool for diagnosing and monitoring this fatal canine disease.

CRediT authorship contribution statement

Nadia Withofs: Writing – review & editing, Supervision, Formal analysis. **Thibault Gendron:** Writing – review & editing, Supervision, Resources, Project administration, Methodology, Investigation. **Mazarine Gérardy:** Writing – review & editing, Methodology, Investigation, Formal analysis. **Géraldine Bolen:** Supervision, Resources, Methodology, Investigation, Formal analysis. **Mohamed Ali Bahri:** Writing – review & editing, Resources, Methodology, Investigation, Formal analysis. **Sylvestre Dammicco:** Writing – review & editing, Resources, Methodology, Investigation, Formal analysis. **Cécile Clercx:** Writing – review & editing, Supervision, Resources, Project administration, Methodology, Investigation, Funding acquisition, Conceptualization. **Elodie Rizzoli:** Writing – review & editing, Writing – original draft, Visualization, Resources, Methodology, Investigation, Formal analysis, Conceptualization. **Christian Degueldre:** Writing – review & editing, Resources, Methodology, Investigation. **Alexandru Tutunaru:** Writing – review & editing, Resources, Methodology, Investigation. **Marie Garigliany:** Writing – review & editing, Supervision, Resources, Methodology, Formal analysis.

Institutional animal care and use committee approval

This study was approved by the animal ethics committee of the University of Liège (approval number 22–2473).

Funding

This study was funded by the Special Research Funds of the Faculty of Veterinary Medicine from the University of Liège and Elodie Rizzoli is a research fellow of the Fonds National de la Recherche Scientifique – FNRS. SOFIE (iTheranostics) provided [^{18}F]FAPI-74 but was not involved in the study design, collection, analysis, interpretation of data and the writing of this article.

Declaration of Competing Interest

The authors declare the following financial interests/personal relationships which may be considered as potential competing interests: Thibault Gendron reports equipment, drugs, or supplies was provided by iTheranostics, Inc. If there are other authors, they declare that they have no known competing financial interests or personal relationships that could have appeared to influence the work reported in this paper

Acknowledgements

The authors gratefully thank Laurie Van Bossuyt, for the technical management of the CT scans; Anne-Christine Merveille and Margaux Legrand for the cardiac ultrasounds for CIPF diagnostic work-up; Gaëlle Schils, for her technical assistance for the PET scans

References

Acharya, P.S., Zukas, A., Chandan, V., Katzenstein, A.-L.A., Puré, E., 2006. Fibroblast activation protein: a serine protease expressed at the remodeling interface in

idiopathic pulmonary fibrosis. Human Pathology 37, 352–360. https://doi.org/10.1016/j.humpath.2005.11.020.
Baum, B., Meneses, F., Kleinschmidt, S., Nolte, I., Hewicker-Trautwein, M., 2007. Age-related histomorphologic changes in the canine Gastrointestinal tract: A histologic and immunohistologic study. World Journal of Gastroenterology 13, 152–157. https://doi.org/10.3748/wjg.v13.i1.152.
Clercx, C., Fastrès, A., Roels, E., 2018. Idiopathic pulmonary fibrosis in West Highland white terriers: An update. The Veterinary Journal 242, 53–58. https://doi.org/10.1016/j.tvjl.2018.10.007.
Corcoran, B.M., Cobb, M., Martin, M.W., Dukes-McEwan, J., French, A., Fuentes, V.L., Boswood, A., Rhind, S., 1999. Chronic pulmonary disease in West Highland white terriers. Veterinary Record 144, 611–616. https://doi.org/10.1136/vr.144.22.611.
Giesel, F.L., Adeberg, S., Syed, M., Lindner, T., Jiménez-Franco, L.D., Mavriopoulou, E., Staudinger, F., Tonndorf-Martini, E., Regnery, S., Rieken, S., El Shafie, R., Röhrich, M., Flechsig, P., Kluge, A., Altmann, A., Debus, J., Haberkorn, U., Kratochwil, C., 2021. FAPI-74 PET/CT Using Either 18F-AlF or Cold-Kit 68Ga Labeling: biodistribution, radiation dosimetry, and tumor delineation in lung cancer patients. The Journal of Nuclear Medicine 62, 201–207. https://doi.org/10.2967/jnumed.120.245084.
Groves, A.M., Win, T., Screaton, N.J., Berovic, M., Endozo, R., Booth, H., Kayani, I., Menezes, L.J., Dickson, J.C., Ell, P.J., 2009. Idiopathic pulmonary fibrosis and diffuse parenchymal lung disease: implications from initial experience with 18F-FDG PET/CT. Journal of Nuclear Medicine 50, 538–545. https://doi.org/10.2967/jnumed.108.057901.
Heikkilä, H.P., Lappalainen, A.K., Day, M.J., Clercx, C., Rajamäki, M.M., 2011. Clinical, bronchoscopic, histopathologic, diagnostic imaging, and arterial oxygenation findings in West Highland White Terriers with idiopathic pulmonary fibrosis. Journal of Veterinary Internal Medicine 25, 433–439. https://doi.org/10.1111/j.1939-1676.2011.0694.x.
Hotta, M., Kim, G.H.J., Rerkpichaisuth, V., Teng, P.Y., Armstrong, W.R., Carlucci, G., Dahlbom, M., Abtin, F., Lari, S.M., Fishbein, G.A., Czernin, J., Volkmann, E.R., Weigt, S.S., Calais, J., 2024. Correlation of FAPI PET uptake with immunohistochemistry in explanted lungs from patients with advanced interstitial lung disease. The Journal of Nuclear Medicine 65, 1789–1794. https://doi.org/10.2967/jnumed.124.268351.
Jayaprakasam, V.S., Paroder, V., Schöder, H., 2021. Variants and pitfalls in PET/CT Imaging of Gastrointestinal Cancers. Seminars in Nuclear Medicine 51, 485–501. https://doi.org/10.1053/j.semnuclmed.2021.04.001.
Laurila, H.P., Rajamäki, M.M., 2020. Update on canine idiopathic pulmonary fibrosis in West Highland White Terriers. Veterinary Clinics of North America: Small Animal Practice 50, 431–446. https://doi.org/10.1016/j.cvsm.2019.11.004.
LeBlanc, A.K., Morandi, F., 2014. Invited review–Off-site PET imaging programs: challenges and opportunities. Veterinary Radiology & Ultrasound 55, 109–112. https://doi.org/10.1111/vru.12103.
LeBlanc, A.K., Peremans, K., 2014. PET and SPECT imaging in veterinary medicine. Seminars in Nuclear Medicine Veterinary Nuclear Medicine 44, 47–56. https://doi.org/10.1053/j.semnuclmed.2013.08.004.
Li, L., Gao, J., Chen, B.-X., Liu, X., Shi, L., Wang, Yanjiang, Wang, L., Wang, Yidan, Su, P., Yang, M.-F., Xie, B., 2023. Fibroblast activation protein imaging in atrial fibrillation: a proof-of-concept study. Journal of Nuclear Cardiology 30, 2712–2720. https://doi.org/10.1007/s12350-023-03352-x.
Lilja-Maula, L.I.O., Laurila, H.P., Syrjä, P., Lappalainen, A.K., Krafft, E., Clercx, C., Rajamäki, M.M., 2014. Long-term outcome and use of 6-minute walk test in West Highland White Terriers with idiopathic pulmonary fibrosis. Journal of Veterinary Internal Medicine 28, 379–385. https://doi.org/10.1111/jvim.12281.
Maitz, C.A., Tate, D., Bechtel, S., Lunceford, J., Henry, C., Flesner, B., Collins, A., Varterasian, M., Tung, D., Zhang, L., Saha, S., Bryan, J.N., 2022. Paired 18F-Fluorodeoxyglucose (18F-FDG), and 64Cu-Copper(II)-diacetyl-bis(N(4)-methylthiosemicarbazone) (64Cu-ATSM) PET scans in dogs with spontaneous tumors and evaluation for hypoxia-directed therapy. Radiation Research 197, 253–260. https://doi.org/10.1667/RADE-20-00186.1.
Mori, Y., Kramer, V., Novruzov, E., Mamlins, E., Röhrich, M., Fernández, R., Amaral, H., Soza-Ried, C., Monje, B., Sabbagh, E., Florenzano, M., Giesel, F.L., Undurraga, Á., 2024. Initial results with [18F]FAPI-74 PET/CT in idiopathic pulmonary fibrosis. European Journal of Nuclear Medicine and Molecular Imaging 51, 1605–1611. https://doi.org/10.1007/s00259-023-06564-y.
Mu, X., Mo, B., Qin, J., Li, Z., Chong, W., Zeng, Y., Lu, L., Zhang, L., Fu, W., 2023. Comparative analysis of two timepoints on [18F]FAPI-42 PET/CT in various cancers. European Journal of Hybrid Imaging 7, 27. https://doi.org/10.1186/s41824-023-00186-1.
Raghu, G., Remy-Jardin, M., Richeldi, L., Thomson, C.C., Inoue, Y., Johkoh, T., Kreuter, M., Lynch, D.A., Maher, T.M., Martinez, F.J., Molina-Molina, M., Myers, J. L., Nicholson, A.G., Ryerson, C.J., Strek, M.E., Troy, L.K., Wijsenbeek, M., Mammen, M.J., Hossain, T., Bissell, B.D., Herman, D.D., Hon, S.M., Kheir, F., Khor, Y.H., Macrea, M., Antoniou, K.M., Bouros, D., Buendia-Roldan, I., Caro, F., Crestani, B., Ho, L., Morisset, J., Olson, A.L., Podolanczuk, A., Poletti, V., Selman, M., Ewing, T., Jones, S., Knight, S.L., Ghazipura, M., Wilson, K.C., 2022. Idiopathic Pulmonary Fibrosis (an Update) and Progressive Pulmonary Fibrosis in Adults: An Official ATS/ERS/JRS/ALAT Clinical Practice Guideline. American Journal of Respiratory and Critical Care Medicine 205, e18–e47. https://doi.org/10.1164/rccm.202202-0399ST.
Randall, E.K., 2016. PET-computed tomography in veterinary medicine (vi). Veterinary Clinics of North America: Small Animal Practice 46, 515–533. https://doi.org/10.1016/j.cvsm.2015.12.008.
Rizzoli, E., de Meeûs d'Argenteuil, C., Fastrès, A., Roels, E., Janssen, P., Puré, E., Garigliany, M.-M., Marichal, T., Clercx, C., 2024. Fibroblast activation protein is a cellular marker of fibrotic activity in canine idiopathic pulmonary fibrosis. Front. Vet. Sci. 11. https://doi.org/10.3389/fvets.2024.1416124.
Roels, E., Couvreur, T., Farnir, F., Clercx, C., Verschakelen, J., Bolen, G., 2017. Comparison between sedation and general anesthesia for high resolution computed tomographic characterization of canine idiopathic pulmonary fibrosis in west highland white terriers. Veterinary Radiology and Ultrasound. https://doi.org/10.1111/vru.12481.
Röhrich, M., Leitz, D., Glatting, F.M., Wefers, A.K., Weinheimer, O., Flechsig, P., Kahn, N., Mall, M.A., Giesel, F.L., Kratochwil, C., Huber, P.E., Deimling, A. von, Heußel, C. P., Kauczor, H.U., Kreuter, M., Haberkorn, U., 2022. Fibroblast Activation Protein-Specific PET/CT Imaging in Fibrotic Interstitial Lung Diseases and Lung Cancer: A Translational Exploratory Study. J Nucl Med 63, 127–133. https://doi.org/10.2967/jnumed.121.261925.
Reinero, C., Visser, L.C., Kellihan, H.B., Masseau, I., Rozanski, E., Clercx, C., Williams, K., Abbott, J., Borgarelli, M., Scansen, B.A., 2020. ACVIM consensus statement guidelines for the diagnosis, classification, treatment, and monitoring of pulmonary hypertension in dogs. Journal of Veterinary Internal Medicine 34, 549–573. https://doi.org/10.1111/jvim.15725.
Syrjä, P., Heikkilä, H.P., Lilja-Maula, L., Krafft, E., Clercx, C., Day, M.J., Rönty, M., Myllärniemi, M., Rajamäki, M.M., 2013. The HistopathOlogy of Idiopathic Pulmonary Fibrosis in West Highland White Terriers shares features of both non-specific interstitial pneumonia and usual interstitial pneumonia in man. Journal of Comparative Pathology 149, 303–313. https://doi.org/10.1016/j.jcpa.2013.03.006.
Thierry, F., Handel, I., Hammond, G., King, L.G., Corcoran, B.M., Schwarz, T., 2017. Further characterization of computed tomographic and clinical features for staging and prognosis of idiopathic pulmonary fibrosis in West Highland white terriers. Veterinary Radiology & Ultrasound 58, 381–388. https://doi.org/10.1111/vru.12491.
van der Gaag, I., 1988. The histological appearance of peroral gastric biopsies in clinically healthy and vomiting dogs. Canadian Journal of Veterinary Research 52, 67–74.
Xu, W., Cai, J., Peng, T., Meng, T., Pang, Y., Sun, L., Wu, H., Zhang, J., Chen, X., Chen, H., 2024. Fibroblast Activation Protein–Targeted PET/CT with 18F-Fibroblast Activation Protein Inhibitor-74 for Evaluation of Gastrointestinal Cancer: Comparison with 18F-FDG PET/CT. Journal of Nuclear Medicine 65, 40–51. https://doi.org/10.2967/jnumed.123.266329.
Yang, P., Luo, Q., Wang, X., Fang, Q., Fu, Z., Li, Jia, Lai, Y., Chen, X., Xu, X., Peng, X., Hu, K., Nie, X., Liu, S., Zhang, J., Li, Junqi, Shen, C., Gu, Y., Liu, J., Chen, J., Zhong, N., Su, J., 2023. Comprehensive Analysis of Fibroblast Activation Protein Expression in Interstitial Lung Diseases. Am J Respir Crit Care Med 207, 160–172. https://doi.org/10.1164/rccm.202110-2414OC.

Glossary

CIPF: canine idiopathic pulmonary fibrosis;
CT: computed tomography;
FAP: fibroblast activation protein;
FDG: fluorodeoxyglucose;
FAPI: fibroblast activation protein inhibitor;
HU: Hounsfield unit;
IPF: idiopathic pulmonary fibrosis;
PET: positron emission tomography;
PET/CT: positron emission tomography combined with computed tomography;
ROI: Region of interest;
SUV: standardized uptake value;
TAV: total active volume;
TBR: target-to-background ratio;
TLV: total lung volume;
WHWT: West Highland white terrier.